Supplement of Atmos. Chem. Phys., 18, 13265–13281, 2018
https://doi.org/10.5194/acp-18-13265-2018-supplement
© Author(s) 2018. This work is distributed under
the Creative Commons Attribution 4.0 License.

Atmospheric Chemistry and Physics
Open Access
EGU

Supplement of

Changes in the aerosol direct radiative forcing from 2001 to 2015: observational constraints and regional mechanisms

Fabien Paulot et al.

Correspondence to: Fabien Paulot (fabien.paulot@noaa.gov)

The copyright of individual parts of the supplement might differ from the CC BY 4.0 License.

Estimate of the variability in the aerosol-free clear-sky outgoing shortwave radiation

We calculate radiative kernels (Soden et al., 2008; Shell et al., 2008) to estimate the change in aerosol-free clear-sky outgoing shortwave radiation (rsutcsaf) due to perturbations in surface albedo (salb), water vapor (WVP), and ozone (qo3). The variability in $rsutcsaf$ is then estimated from $(\alpha \cdot salb + \beta \cdot WVP + \gamma \cdot qo3)\, swdn$ where $\alpha = \frac{\partial palb}{\partial salb}$, $\beta = \frac{\partial palb}{\partial WVP}$ and $\gamma = \frac{\partial palb}{\partial qo3}$. swdn and palb are the incoming shortwave flux at the top of the atmosphere and the planetary albedo, respectively. The α, β, and γ radiative kernels are derived using the AM3 radiative model.

We evaluate our methodology by comparing the annual variability of rsutcsaf calculated in CERES SYN over the 2001-2015 period with that estimated using the radiative kernels introduced above. CERES SYN rsutcsaf is calculated using surface albedo, water vapor, and ozone constrained by observations inputted into a radiative transfer code. We use the same surface albedo, water vapor, and ozone in conjunction with our Jacobian to estimate the variability in rsutcsaf. Figure S1 shows the root mean square (RMS) of the annual anomaly in rsutcsaf from SYN (panel A) and how it is reduced by applying in succession the correction terms for surface albedo ($\alpha \cdot salb$), water vapor ($\beta \cdot WVP$), and ozone ($\gamma \cdot qo3$). Correcting for changes in the salb reduces the RMS over most land regions (Figure S1B). However, the RMS remains large over the Sahara, Australia, the Amazon, and North America. It is further reduced once changes in water vapor and to a lesser extend ozone are accounted for (Figure S1C and D).

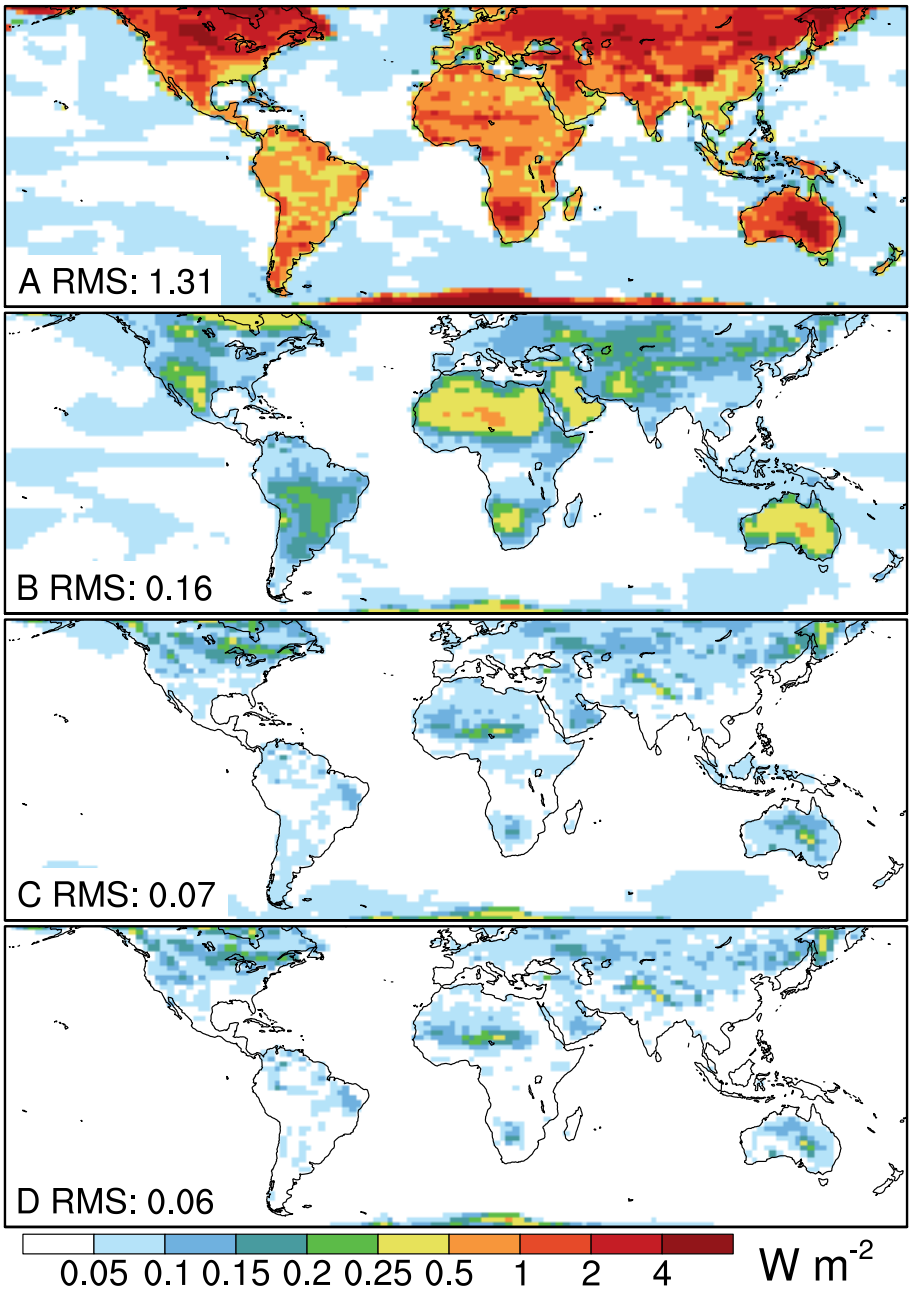

Figure S1: Root mean square of the annual anomaly in the outgoing clear-sky shortwave radiation without aerosols (Rsutcsaf) and its decrease after accounting for the effect of albedo (B), albedo and water vapor (C), albedo, water vapor, and ozone (D). The area weighted RMS over land from 60S to 60N is in indicated in each panel

Table S1: Observation-based and simulated estimates of the decadal trend in DRE^{sw}_{clr} ($W\,m^{-2}\,decade^{-1}$) in selected regions from 2001 to 2015[a]

	$EBAF_R$		SYN		$EBAF_C$		$EBAF_M$		AM3	
Eastern US	*	*	1.8	[1.2 2.1]	1.4	[1.0 1.7]	0.9	[0.6 1.4]	0.8	[0.6 0.9]
Western Europe	*	*	1.4	[1.2 1.6]	1.0	[0.7 1.1]	0.7	[0.4 0.8]	0.6	[0.3 0.8]
India	0.5	[0.2 0.7]	-1.9	[-2.2 -1.2]	-1.5	[-1.9 -1.2]	-1.0	[-1.3 -0.6]	-2.4	[-2.7 -2.2]
Eastern China	-0.8	[-1.4 -0.4]	*	*	*	*	*	*	-1.3	[-1.7 -0.9]

[a] The trend is estimated using the Theil-Sen method. Bootstrap estimates of the 95% confidence interval are indicated in bracket. * denote non significant monotonous change at p=0.05

Table S2: Observation-based and simulated decadal trends for the AOD and direct clear-sky shortwave radiative effect (DRE^{sw}_{clr}, W m^{-2} decade^{-1}) for selected regions and seasons from 2002 to 2015[a]

	Western Europe		Eastern US		India		Eastern China
	MAM	JJA	MAM	JJA	DJF	MAM	MAM
AOD							
MODIS (TERRA)	-0.04 [-0.05,-0.02]	-0.04 [-0.07,-0.02]	-0.04 [-0.06,-0.01]	-0.11 [-0.16,-0.09]	0.13 [0.10,0.16]	0.04 [0.00,0.07]	* [-0.04,0.07]
MODIS (AQUA)	-0.05 [-0.06,-0.02]	-0.03 [-0.05,-0.02]	-0.04 [-0.06,-0.01]	-0.10 [-0.17,-0.07]	0.11 [0.08,0.15]	0.07 [0.03,0.09]	* [-0.08,0.08]
MISR	-0.03 [-0.04,-0.02]	-0.03 [-0.06,-0.02]	-0.02 [-0.04,-0.01]	-0.08 [-0.12,-0.07]	0.05 [0.03,0.07]	* [0.01,0.05]	
MATCH	-0.06 [-0.07,-0.04]	-0.06 [-0.10,-0.05]	-0.07 [-0.10,-0.05]	-0.11 [-0.15,-0.10]	0.10 [0.07,0.13]	0.03 [0.01,0.06]	* [-0.07,0.12]
AM3	-0.04 [-0.05,-0.01]	-0.05 [-0.08,-0.03]	-0.03 [-0.05,-0.01]	-0.05 [-0.07,-0.04]	0.13 [0.10,0.17]	0.15 [0.11,0.18]	0.15 [0.12,0.22]
DRE^{sw}_{clr}							
SYN	1.8 [1.3,2.2]	2.5 [2.0,3.2]	2.1 [1.3,2.7]	3.6 [3.0,4.4]	-2.6 [-3.3,-2.1]	-1.4 [-2.2,-0.6]	* [-1.7,1.5]
$EBAF_C$	1.4 [0.6,1.6]	1.8 [1.5,2.4]	1.3 [0.5,2.2]	3.3 [2.7,4.2]	-2.3 [-3.2,-2.1]	-1.2 [-2.2,-0.6]	* [-1.7,0.8]
$EBAF_M$	1.0 [0.3,1.3]	1.2 [1.0,1.7]	* [-0.0,1.5]	2.0 [1.1,3.1]	-0.8 [-1.6,-0.6]	-0.9 [-1.2,-0.4]	* [-1.4,0.7]
AM3	1.1 [0.3,1.2]	1.5 [0.9,2.2]	0.9 [0.5,1.2]	1.4 [1.2,2.0]	-2.7 [-3.2,-2.2]	-3.1 [-3.9,-2.6]	-2.1 [-3.5,-1.6]

[a] The trend is estimated using the Theil-Sen method. Bootstrap estimates of the 95% confidence interval are indicated in bracket. * denote non significant monotonous change at p=0.05

Table S3: Observation-based estimates and simulated decadal trends in surface broadband albedo from 2002 to 2015 over India[a] ($decade^{-1}$)

	DJF	MAM
SYN	-9.6×10^{-3}[0.129]	-8.7×10^{-3}[0.128]
EBAF	-1.3×10^{-2}[0.135]	-9.9×10^{-3}[0.131]
MODIS	-6.1×10^{-3}[0.158]	-7.5×10^{-3}[0.163]
AM3	-2.6×10^{-3}[0.166]	* [0.151]

[a]The average over the period 2002–2015 is shown in bracket. Trend is estimated using the Theil-Sen method. * denotes non significant monotonous change at p=0.05. SYN, EBAF, and MODIS refer to CERES SYN, CERES EBAF, and MODIS albedo, respectively

Table S4: Aerosol radiative forcing under all-sky and clear-sky conditions for 2001 relative to 1850 [a]

	All-Sky		Clear-Sky	
Anthropogenic dust	-0.01	[-0.05[c]]	-0.09	[-0.07[c]]
Organic Carbon	-0.06	[-0.09[b],-0.06[c]]	-0.10	[-0.08[c]]
Sulfate	-0.43	[-0.32± 0.15[b],-0.28[c]]	-0.73	[-0.38[c]]
Nitrate	-0.05	[-0.08±0.04[b],-0.071[c]]	-0.08	[-0.10[c]]
Black Carbon	0.45	[0.18±0.07[b],0.08[c]]	0.36	[0.06[c]]
Total	-0.09	[-0.27±0.15[b],-0.36[c]]	-0.64	[-0.67±0.18[b],-0.57[c]]

[a] in $\mathrm{W\,m^{-2}}$

[b] Brackets denote estimates from the AEROCOM project for year 2000 (Myhre et al., 2013)

[c] Heald et al. (2014) for 2010

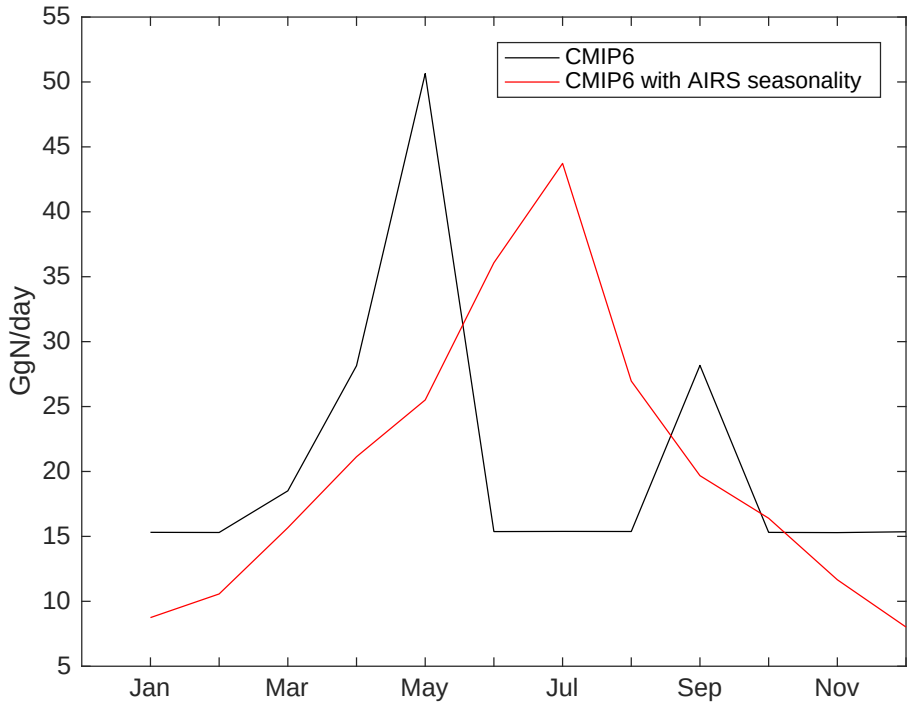

Figure S2: CMIP6 ammonia emissions for India with seasonality from CMIP6 (black) and AIRS (red)

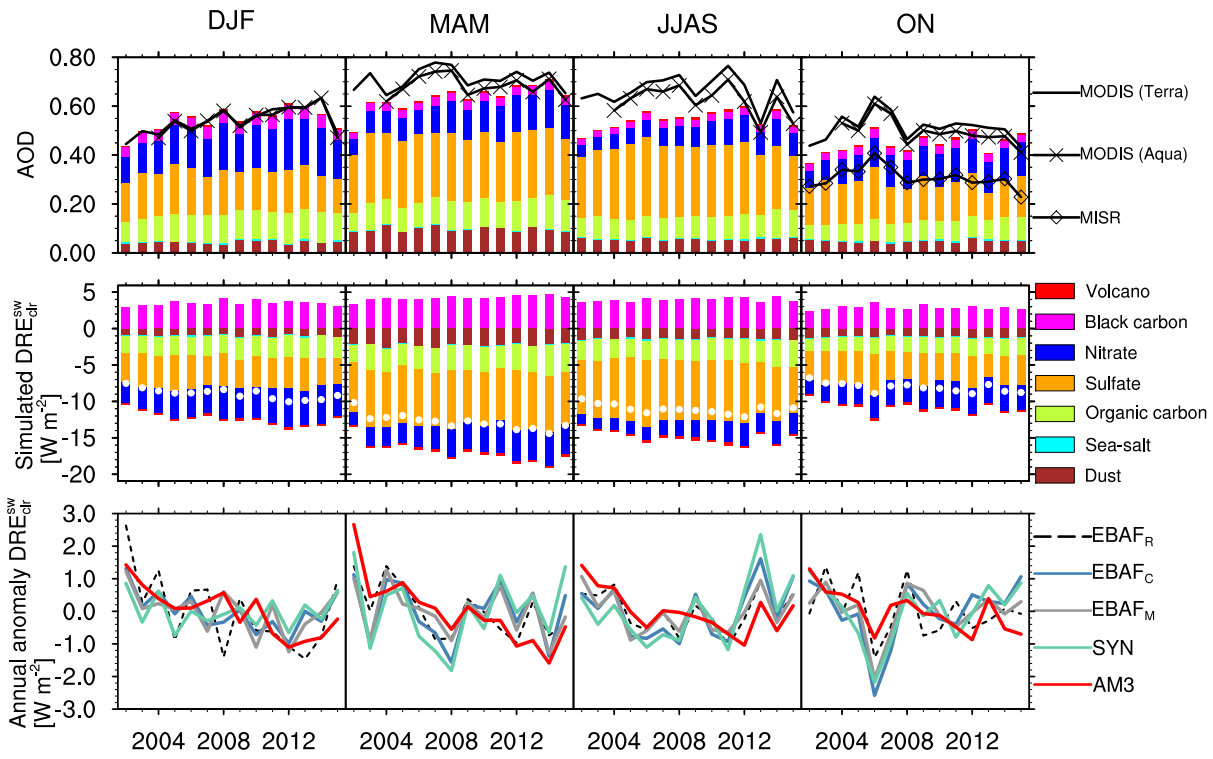

Figure S3: Seasonal changes in the aerosol optical depth (AOD) and clear-sky shortwave aerosol direct radiative effect (DRE^{clr}_{sw}) in Eastern China (Fig. 3) using MEIC emissions over China (see text). The top row shows the AOD retrieved from different spaceborne instruments (MODIS-Terra (lines), MODIS-Aqua (cross), MISR (diamond)) and the simulated AOD decomposed into its components (bars). The second row shows the simulated clear-sky shortwave aerosol direct radiative effect of individual aerosols (bars) and the overall aerosol direct radiative effect (white circle). The bottom row shows observation-based and simulated estimates of changes in the aerosol direct radiative effect.

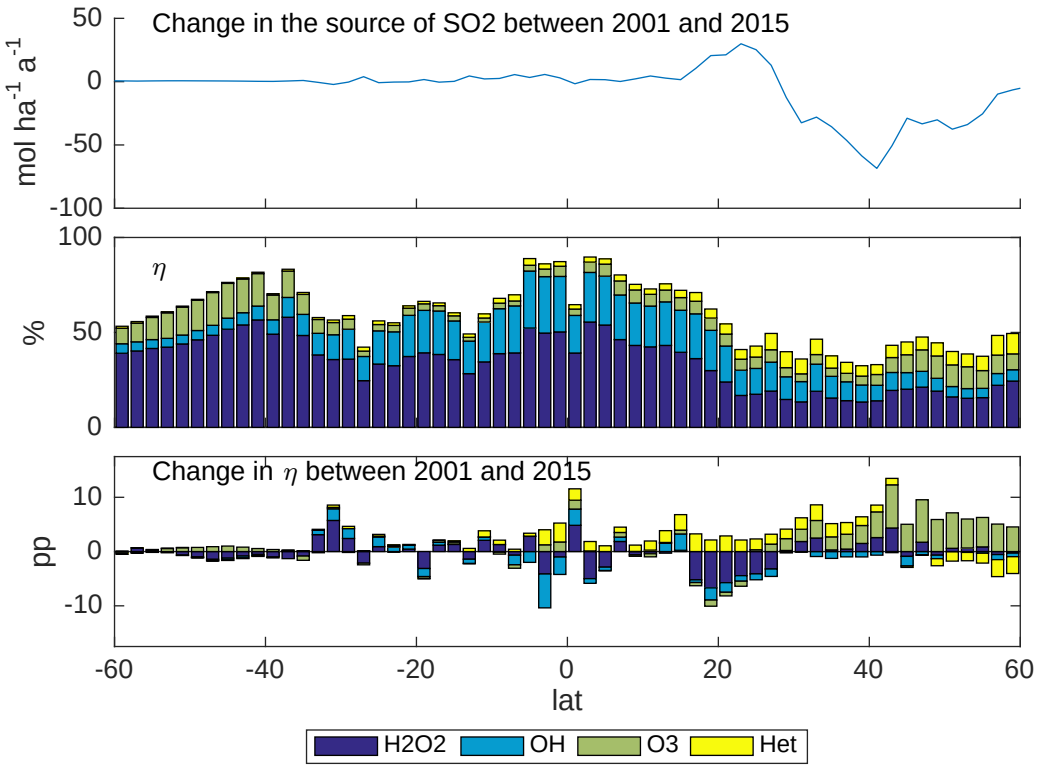

Figure S4: Meridional change in the source of SO_2 (top), conversion efficiency (η) between SO_2 and SO_4^{2-}, and change in η from 2001 to 2015

References

Heald, C. L., Ridley, D. A., Kroll, J. H., Barrett, S. R. H., Cady-Pereira, K. E., Alvarado, M. J., and Holmes, C. D.: Contrasting the direct radiative effect and direct radiative forcing of aerosols, Atmos. Chem. Phys., 14, 5513–5527, doi:10.5194/acp-14-5513-2014, URL http://www.atmos-chem-phys.net/14/5513/2014/, 2014.

Myhre, G., Samset, B. H., Schulz, M., Balkanski, Y., Bauer, S., Berntsen, T. K., Bian, H., Bellouin, N., Chin, M., Diehl, T., Easter, R. C., Feichter, J., Ghan, S. J., Hauglustaine, D., Iversen, T., Kinne, S., Kirkevåg, A., Lamarque, J.-F., Lin, G., Liu, X., Lund, M. T., Luo, G., Ma, X., van Noije, T., Penner, J. E., Rasch, P. J., Ruiz, A., Seland, Ø., Skeie, R. B., Stier, P., Takemura, T., Tsigaridis, K., Wang, P., Wang, Z., Xu, L., Yu, H., Yu, F., Yoon, J.-H., Zhang, K., Zhang, H., and Zhou, C.: Radiative forcing of the direct aerosol effect from AeroCom Phase II simulations, Atmos. Chem. Phys., 13, 1853–1877, 2013.

Shell, K. M., Kiehl, J. T., and Shields, C. A.: Using the Radiative Kernel Technique to Calculate Climate Feedbacks in NCAR's Community Atmospheric Model, Journal of Climate, 21, 2269–2282, doi:10.1175/2007jcli2044.1, URL https://doi.org/10.1175/2007jcli2044.1, 2008.

Soden, B. J., Held, I. M., Colman, R., Shell, K. M., Kiehl, J. T., and Shields, C. A.: Quantifying Climate Feedbacks Using Radiative Kernels, Journal of Climate, 21, 3504–3520, doi:10.1175/2007jcli2110.1, URL https://doi.org/10.1175/2007jcli2110.1, 2008.